Published in final edited form as:
J Cardiovasc Transl Res. 2013 August ; 6(4): 623–639. doi:10.1007/s12265-013-9461-4.

EVALUATION OF RIGHT AND LEFT VENTRICULAR DIASTOLIC FILLING

Ares Pasipoularides, MD, PhD, FACC
Consulting Professor of Surgery, Duke University School of Medicine. Formerly, Director of Cardiac Function, Duke/NSF Center for Emerging Cardiovascular Technologies. Durham, N.C. 27710, USA. Duke University School of Medicine. HAFS - 7th floor, DUMC 3704, Durham, NC 27710, United States. 828-254-0279

Ares Pasipoularides: apasipou@duke.edu

Abstract

A conceptual fluid-dynamics framework for diastolic filling is developed. The *convective deceleration load* (CDL) is identified as an important determinant of ventricular inflow during the *E*-wave (*A*-wave) upstroke. Convective deceleration occurs as blood moves from the inflow anulus through larger-area cross-sections toward the expanding walls. Chamber dilatation underlies previously unrecognized alterations in intraventricular flow dynamics. The larger the chamber, the larger become the endocardial surface and the CDL. CDL magnitude affects strongly the attainable *E*-wave (*A*-wave) peak. This underlies the concept of *diastolic ventriculoannular disproportion*. Large vortices, whose strength decreases with chamber dilatation, ensue after the *E*-wave peak and impound inflow kinetic energy, averting an inflow-impeding, convective Bernoulli pressure-rise. This reduces the CDL by a variable extent depending on vortical intensity. Accordingly, the filling vortex facilitates filling to varying degrees, depending on chamber volume. The new framework provides stimulus for functional genomics research, aimed at new insights into ventricular remodeling.

Keywords

diastolic filling vortex; ventricular chamber volumes; diastolic function; heart failure; ventricular remodeling; convective deceleration load; diastolic ventriculoannular disproportion; functional genomics of intracardiac blood flow

---

"Cardiology is flow." Richter Y. & Edelman E.R. (2006). *Circulation* 113, 2679.

Diastolic cardiac dysfunction as a component of heart failure is nowadays sufficiently recognized as to be a part of coding for congestive heart failure (CHF) in the International Classification of Diseases (ICD-10, codes I50.30–33). This WHO recognition of diastole has been accompanied by major strides in the appraisal of diastolic function [1–4], made possible by technology encompassing multisensor cardiac catheterization [1,2,5,6] and new digital imaging modalities [1,6–8]. It is now widely appreciated that enhancing diastolic filling has clinical merit and that the significance of diastolic dysfunction is far reaching [9]. Nonetheless, the fact that in health and disease diastolic dynamics are dependent on a large number of factors and their interactions [1,10] has complicated evaluation of the multifactorial causes of the observed ventricular filling abnormalities.

Conflict of interest The author declares that he has no conflict of interest.

Remodeling with ventricular enlargement has surfaced as a central mechanism, relevant to heart failure progression and to prediction of outcomes, as pathophysiologic understanding of heart failure has progressed in the past 3–4 decades [1]. In primary systolic myocardial dysfunction and failure, ventricular enlargement occurs and entails a greater increase in transverse than in long chamber-axis (sphericalization). In primary diastolic myocardial dysfunction, the ejection fraction is normal or higher than normal and chamber size is unchanged or decreased. Most intriguing is that ventricular diastolic function is frequently abnormal in patients with primary systolic dysfunction and failure. The present survey considers evidence that besides leading to increased wall stresses and impaired systolic function [11,12], ventricular chamber enlargement *per se* hampers diastolic filling, thus impairing ventricular diastolic function.

This viewpoint stems from integrative research findings and concepts, which pertain to interactions of cardiac fluid dynamic mechanisms with atrioventricular (A-V) dynamic geometry and inflow patterns, and from diastolic function alterations accompanying chamber enlargement in animal models of heart disease and failure [6,8,13–17]. The clinical studies that we will review, which confirm the underlying fluid dynamics principles, also demonstrate the value of these simple but useful principles in managing heart failure with remodeling and chamber dilatation.

Ventricular enlargement does not impair myocardial diastolic function

Ventricular diastole encompasses two main features determining dynamics: *relaxation* and *compliance*. The interplay between all the factors determining ventricular filling is complex and quite protean, reflecting continual adaptation to shifts in the operating environment (see Fig. 1). The inflow velocity time course, in particular, may be affected by changes in myocardial relaxation and ventricular compliance properties, atrial pressure and compliance, and atrioventricular valvular morphology. Inflow valve opening in the physical sense and the onset of rapid ventricular filling coincide well with the instant of reversal of the atrioventricular pressure difference across the atrioventricular valve cusps [1]: blood rushes into each ventricle, which is at its end systolic volume (ESV). Early diastolic filling is rapid because of continuing ventricular relaxation with declining RV/LV chamber pressures. At normal or abnormally low heart rates, the rapid ventricular filling phase evolves into the slow filling phase; at high normal or abnormally fast rates, it *merges* with the active filling that is caused by atrial systole. The initial phase of the translational research, which led to the integrative diastolic function framework that is depicted in Fig. 1, entailed baseline and longitudinal studies on subacute-to- chronic canine surgical models of RV volume overload (VO), pressure overload (PO) and myocardial ischemia (IS); we utilized right-heart multisensor Millar catheters, real-time 3-D echocardiography, and specially designed pulse-transit ultrasonic dimension transducers [8,18,19]. Only chronically instrumented awake dogs were studied, because of important limitations of acute studies under conditions of anesthesia, recent surgery, and open-chest [18,20,21].

Changes from control ensuing in myocardial and ventricular diastolic active and passive wall mechanics in the animal disease models are presented and discussed in detail in a companion paper in *JCTR* [22]. Here, I will summarize next relevant findings regarding myocardial relaxation dynamics and passive filling pressure vs. volume relations and myocardial compliance. First I must note that *early* diastolic filling is normally dominant (*E*-wave), with a supplementary increment associated with atrial contraction (*A*-wave). The main influences on early ventricular inflow rate and volume pertain to myocardial relaxation dynamics and are different from those affecting late filling which commonly relate to passive ventricular and myocardial compliance.

Myocardial relaxation dynamics

The processes going on during the early filling period are neither purely passive nor purely active. This led me by 1980 to postulate that total measured left ventricular diastolic pressure (P_M) is determined by two overlapping processes, namely, the *myocardial relaxation*-induced decay of actively developed pressure, (P_R); and, the concurrent *buildup* of passive filling pressure (P*), and to develop a comprehensive mathematical model for diastolic dynamics, as I have detailed in a recent survey [10]. Further application of this model has allowed comprehensive evaluations of the role of active and passive dynamic factors in diastolic ventricular mechanics in health and disease [1,2,10,22].

$$P_R = P_0 \bullet \exp(-t/\tau) + P_b \quad \text{(Eq. 1)}$$

An exponential model (Eq. 1) characterized accurately the decay of isovolumic RV pressure, P_R, with three parameters: P_0, τ, and P_b. The time constant of relaxation, τ (tau), is the most important among them; it quantifies the *rate of myocardial relaxation* and pressure decay with the reuptake of Ca^{2+} (which when bound to troponin C allows the crossbridge movement of the myofibrils resulting in force development and contraction) by the sarcoplasmic reticulum [23]. P_b is also important, because it represents the asymptotic level to which the pressure would tend, if the decaying process were allowed to proceed indefinitely. Finally, when the pleural pressure does not deviate significantly from zero, the parameter P_0 is indicative of the beginning level of the exponential isovolumic pressure decay. As is shown in Table 1, in contrast to pressure overload and myocardial ischemia, no significant change from control was found with VO and the resultant chamber enlargement [18,22] in the RV time constant of relaxation, τ [18,22]. The only significant change in VO was a raised RV diastolic pressure asymptote, P_b, reflecting increased diastolic constraint from elevated right heart volumes [1,2,18,21,23]. These findings suggest that the relaxation mechanism is unimpaired in subacute-to-chronic RV volume overload with chamber dilatation and does not adversely impact ventricular filling [18]. They are consistent with earlier LV findings by Zile and co-workers on a comparable canine VO model [24], and with subsequent clinical findings in children with diverse conditions producing RV volume overload and chamber enlargement [25].

Filling pressure vs. volume relationships

A sigmoidal model [1,19,22] for passive filling pressure vs. volume relations and the resultant myocardial compliance formulations showed that the maximum RV myocardial compliance, which is attained during early filling, was reduced significantly from control with pressure overload and ischemia but not with VO. Statistical analyses, including ANOVA and Bonferroni- Holm statistics, were performed on the impact of each disease modality on model parameters and indexes of RV diastolic function. Important changes in passive filling pressure vs. volume relations and diastolic properties are induced by the three disease modalities (see Table 2). As is shown in Table 2, PO alters myocardial compliance properties substantially. It caused a decrease in maximum RV myocardial compliance as well as an increase in passive filling pressure levels at both maximum and end-diastolic myocardial compliance. IS also decreased considerably the maximum compliance that was attained during the early filling process. Therefore, both PO and IS impaired myocardial compliance [19,22] and diastolic filling. On the contrary, VO with chamber enlargement exhibited only a slightly decreased maximal compliance and a strikingly strong *increase* in end-diastolic myocardial compliance [19,22] compared to control (see Table 2), which implies *no* impairment of diastolic ventricular function [2,19,22]. In contrast to pressure overload and ischemia, in VO the pressure-volume relationship shifts far to the right and downward over much of the filling process [1,19,22]; thus, end-diastolic myocardial

compliance actually increased in VO with chamber enlargement compared to control, while end-diastolic pressure was unchanged. These RV results are again congruous with LV data obtained on a similar VO canine model, by Zile and co-workers [24].

Fluid dynamic underpinnings for filling impairment in dilated ventricles

The intriguing feature of the foregoing findings was that eccentric hypertrophy (chamber enlargement) consequent to VO resulted in minimal abnormalities relative to control in myocardial properties. Since the RV chamber size in VO (EDV, 60 ± 29 ml) increased markedly ($P<0.05$) from control (45 ± 21 ml), reflecting elongation and "slippage" of myocytes within the wall contributing to myocardial creep and remodeling [1,19,22], it was hypothesized that it might be responsible for unrecognized functional filling dynamics changes relative to control. Therefore, it became apparent that a fuller understanding of integrative diastolic function in chamber enlargement would be forthcoming only by expanding the scope of the investigations beyond myocardial mechanics, which consider exclusively myocardial relaxation and wall compliance changes affecting diastolic ventricular function.

A comprehensive examination of ventricular filling was therefore undertaken, utilizing combined sonomicrometric, digital imaging, and computational fluid dynamics (CFD) methods, to look for fluid dynamic underpinnings of diastolic dysfunction in enlarged ventricles [8,13,14,17]. Such mechanisms would significantly alter the prevalent understanding of factors contributing to diastolic filling impairment in heart failure with remodeling.

The Functional Imaging method for visualizing intracardiac flow

The ensuing fluid dynamics studies [8,13,14] revealed important but previously unrecognized mechanisms responsible for the filling impairment in the volume-overloaded, dilated ventricles. These underlying mechanisms were revealed and investigated by the Functional Imaging (FI) method [1,8]. The method comprises real-time, 3-D echocardiographic (RT3D) and sonomicrometric measurements, combined with computational fluid dynamics simulations of the intracardiac flow field [1,6,16,17]. It was applied to ascertain diastolic filling dynamics in individual dogs, studied at control and with chamber enlargement induced by RV subacute-to-chronic VO. With the use of Functional Imaging [8], our investigations [13,14] were the first to show in detail the kinematic and dynamic characteristics of the diastolic filling vortex inside the *right* ventricle. Its LV counterpart had already been shown in the pioneering investigations of Taylor and Wade and Bellhouse (see below).

Although RT3D images [1,8] were used in these studies, the pertinent techniques are applicable generally to modern digital imaging methods [7,26–31]. Robert Hooke, the English Leonardo Da Vinci, had argued in his *Micrographia* that scientific progress would depend on replacing or reinforcing weak human senses with mechanical or optical devices (32). Paraphrasing today, we see that translational scientific progress depends, in large measure, on state-of-the-art visualization methods. The FI method yields values of velocity and pressure at literally thousands of discrete points in space and time within each filling chamber simulated. The acquired vast amounts of qualitative and quantitative spatiotemporal information can be envisaged effectively only when transformed into graphic representations (cf. the example in Fig. 4, bottom panels). Accordingly, high-resolution plots of instantaneous intraventricular velocity and pressure distributions were extracted from the FI simulation datasets, using interactive graphics modules [1,6,8,13–17]. They reveal time-dependent, subtle interactions (see below) between the local acceleration and the convective acceleration components of the total pressure gradient [1,6,14]. Not only does the smallness

of the directly measurable total early diastolic intraventricular pressure gradients render most d i r e c t measurements—even by solid-state multisensor catheter—unreliable but, until the comprehensive studies surveyed here [6,8,13–17] this smallness also concealed the clinically noteworthy fluid dynamics mechanisms underlying these gradients [1,6].

Local and convective acceleration components of instantaneous flow velocity

Just as during ejection [5], in the intraventricular diastolic flow field the velocity is a function of both time and space [6]. Generally, there can be acceleration of fluid passing through a point even when the velocity at the given point is constant, i.e., even if the *local* acceleration is zero [1,5,6,33–35]. Streamlines connect velocity vectors in a flow field and show the direction a fluid element is traveling in at a given instant; a tangent to a streamline at any point is parallel to the fluid's instantaneous velocity at that point. When streamlines are plotted so that the distances between them correspond to equal volumetric *flux* (integration of the *flux* over the distance between adjacent streamlines gives the volumetric flow rate), the resulting plot gives information about regions of high and low velocities [36,37]. Simply put, closely spaced streamlines indicate relatively high linear velocities, and vice-versa. Converging streamlines in a flow region imply *convective* (flow-associated) *acceleration*; diverging streamlines imply *convective deceleration* along the stream (see Figs. 1 and 2) [1,5,13,14,35,36].

Atrioventricular transvalvular and intraventricular diastolic pressure gradients

Tricuspid transvalvular phasic pressure differences were measured by multisensor right-heart catheters under experimental hyperdynamic conditions, which accentuate them, and were found [1,6,14] to possess dynamic characteristics, including their timing relative to the inflow velocity, similar to those derived and validated for the mitral transvalvular pressure drop using clinical human data by Mirsky and Pasipoularides [2] and Isaaz [38]. Instantaneous RV intraventricular diastolic pressure gradients are smaller [1,6,14] than their LV counterparts and are not generally amenable to reliable direct measurement by catheter, as noted above.

The FI method has shown [1,8,13–17] that up to the *E*-wave peak, instantaneous inflow streamlines extend from the tricuspid orifice to the RV endocardial surface in an expanding fan-like pattern (Fig. 1, right). Consequently, the RV inflow is undergoing a convective deceleration, similar to the early diastolic LV inflow deceleration found in humans by Houlind et al. [39] in meticulous investigations using three-directional velocity-encoded MRI. During the *E*-wave upstroke, the total instantaneous intraventricular pressure gradient along the inflow stream is the algebraic sum of a streamwise (i.e., in the flow direction) pressure fall contributed by the local acceleration, and a Bernoulli pressure-rise contributed by the convective deceleration. This streamwise Bernoulli pressure-rise counterbalances partially the pressure fall engendered by the simultaneously applying local acceleration of the inflow [1,6,14].

Convective deceleration load (CDL)

The preceding mutually *offsetting* action underlies the peculiar smallness of the total early diastolic intraventricular pressure gradients in animals and humans [1,2,6,14,40]. During ejection, on the other hand, throughout the upstroke of the ejection waveform both the convective and the local intraventricular acceleration effects act in the same sense [1,5,6,12,32,35], actually *reinforcing* each other. These contrasting dynamics of its components under normal conditions underscore the much less prominent *total* (measured by multimicromanometric catheter [1,2,5,6]) intraventricular diastolic pressure gradient during the upstroke of the *E*-wave, even under hyperdynamic conditions, such as during

exercise, when both convective and local acceleration components are augmented and do accentuate strongly the total *ejection* gradient [1,5,33].

At peak volumetric inflow the local acceleration vanishes and the total intraventricular gradient is represented by the convective component which is *adverse*; i.e., the flow encounters *higher* pressures as it moves downstream. Flow persists under its previously built-up momentum [14], just as forward vehicle motion persists transiently after applying the brakes. These considerations led to the formulation of a new mechanism, the *"convective deceleration load"* (CDL) [1,6,8,13–15,17], as an important determinant of diastolic inflow and its hemodynamic impairment in presence of chamber enlargement, as is detailed below.

Diastolic ventriculoannular disproportion and clinical indicators of elevated CDL

Clinically, the magnitude of CDL affects strongly the attainable peak *E*-wave velocities while, simultaneously, CDL itself is being affected strongly by them. Furthermore, the pressure-rise representing CDL is proportional to the *square* of the applying inflow velocities. This is simply a consequence of the familiar Bernoulli principle, which shows that the convective acceleration- or deceleration-induced changes in pressure are proportional to the square of the applying reference velocity [1,5]. Consequently, diastolic filling difficulties attributable to an augmented CDL will be exacerbated under any (patho) physiologic states that are characterized by increased ventricular inflow velocities; e.g., during exercise or stress.

Moreover, the bigger the ventricle, the larger becomes the ratio of the inner-surface area of the chamber to the area of the inflow annulus, and the higher the convective deceleration and the CDL (Fig. 1, right). It is necessary to bear in mind that the discrepancy in the two areas involved is greatly underestimated by envisaging 2-D axial sections through the actually three-dimensional flow field.—To ascertain this generally unappreciated fact, please refer to Fig. 2. Accordingly, an enlarged (e.g., dilatation in failure) ventricle at end-systole/early diastole provokes a disproportionate increase of CDL and more difficult diastolic inflow [1,6,8,13–15,17]. More specifically, it is abnormally raised end-systolic or, equivalently, earlydiastolic volumes that matter; this is considered further later on, in the section titled "Clinical implications for diastolic filling in dilated ventricles." Difficulties accruing from pathologic ESV elevations can be exacerbated by tachycardia, which commonly accompanies systolic dysfunction and failure and causes diastolic filling time to wane. Of course, in normal subjects tachycardia elicited by adrenergic mechanisms decreases ESV. Cardiac resynchronization therapy (CRT) [41,42,43] can reduce ESV in patients with primary systolic dysfunction and failure; thus, it should reduce the CDL and mitigate the secondary impairment in diastolic filling and function.

Clinically, augmentation of CDL may contribute to depressed *E*-wave amplitudes and *E/A* ratio abnormalities, and to elevated atrial pressures and upstream congestion in acute or chronic heart failure with chamber dilatation. Ensuing atrial overload (active compensation for difficult ventricular filling by strong atrial myocardial contraction) may account for the association of atrial fibrillation (AF) with clinical ventricular enlargement in absence of coronary disease, especially in elderly subjects [14]. This is especially relevant today, with the rising proportion of the elderly in the population. The loss of the "atrial kick" in AF can have severe repercussions under conditions of increased CDL with diastolic filling impairment.

The greater the discrepancy between the sizes of the RV/LV endocardial surface and the atrioventricular (AV) valve anulus, the larger becomes the CDL—Fig. 2. This consideration underlay the formulation [1,8,13–15,17] of the clinically important concept of a *"diastolic ventriculoannular (inflow valve) disproportion"* (see DVAD in Fig. 1, right), which is the

counterpart, or diastolic analog, of the *"systolic ventriculoannular (outflow valve) disproportion,"* formulated in a systolic clinical fluid dynamics survey in *JACC* [5].

Diastolic large-scale intraventricular vortical motions

Early on during the downstroke of the *E*-wave, the intraventricular t o t a l pressure gradient becomes strongly adverse: it now embodies pressure augmentations in the downstream flow direction accruing from *both* local and convective decelerations [1,6,13,14]. This induces flow instability and large-scale vortical motions, (Fig. 1, right). Details on the formation and evolution of the intraventricular diastolic filling vortices are presented elsewhere [1]; Fig. 3 epitomizes graphically the clinically important concepts. Relevant here are the classic discoveries of Taylor and Wade, in dogs and sheep; using cineradiography with fine stream dye injection, and endoscopic cinephotography, these pioneers demonstrated vortex formation in both the right and left ventricles during diastolic filling [44]. They agree also with contemporary systematic clinical measurements of Rodevand et al. [45] in the left ventricle: using Doppler echocardiography techniques, they showed that during early transmitral flow acceleration, all intraventricular velocities are directed toward the chamber walls; however, after the peak of the *E*-wave retrograde velocities ensue around the central inflow, reflecting large-scale vortical flow [1,45].

Large-scale (of a size comparable to that of the RV or the LV chamber) vortices dissipate little flow energy by viscous (frictional) effects. However, interactions of these vortices with each other generate intermediate- and small-scale eddies, which are strongly dissipative. Thus, there is a cascade of energy from large, through intermediate, to small eddies, where rotational kinetic energy is dissipated as heat [1,10,13].

Spanish investigators, in collaboration with scientists at the University of California San Diego, have recently been studying how heart rate and AV synchronicity influence vortex kinematics, using 2-D, B-mode and conventional color-Doppler sequences of the full LV, obtained from an apical long-axis view [46,47]. Initial results, in patients with an implantable cardiac resynchronization device, indicate that the duration of diastole, as modulated by heart rate and AV-delay, modifies significantly intraventricular vortex kinematics.

Visualization of the diastolic filling vortex

The diastolic vortex is considerably more intense in the normal-sized than in the dilated chamber [1,13,14,17], as is nicely demonstrated in the color mappings offered in Fig. 4 (lower panels), which were obtained by the FI method [8,13]. Comparable color mappings are familiar to echocardiographers and are appropriate for revealing the global organization of intracardiac flows. The regions with red and orange colors represent blood flow toward the base of the ventricle, whereas regions with blue and green colors represent blood flow toward the apex. The intense *deceleration* of the flow in the proximate vicinity of the *inflow* anulus is striking; it will be discussed further in conjunction with the plots of velocity vs. axial distance from the inflow anulus in Fig. 5. At this juncture, it is interesting to note that, contrariwise during ejection, in the close vicinity of the *outflow* valve anulus there is invariably intense convective *acceleration* of the flow [1,5,33–36]. These concentrated convective velocity changes in the vicinity of circular 2-D inflow/outflow anuli are related to the 3-D ventricular flow field geometry (see Fig. 2)—as is also the "inverse-square law" of physics for, e.g., sound intensity vs. distance from its source.

Vortices represent rotatory motions of a multitude of fluid particles around a common center and rotating flows have fascinated people for centuries. Leonardo da Vinci studied, drew, and described accurately vortices within the sinuses of Valsalva in his *Quaderni d'*

Anatomia, which was published in 1513 [1,5], a century before Harvey's discovery of the circulation of blood.

Bellhouse's model studies of the effect of chamber size on vortex strength and AV valve closure

Diastolic LV vortices are well visualized using cardiac MRI and color Doppler-based echocardiographic vector flow mapping [1,26–30]. Their fluid dynamics were investigated in pioneering studies on mechanical analogs of the left heart by Bellhouse [48]. He observed that the mitral valve leaflets opened wide early in diastole, then moved increasingly toward closure, and were almost fully apposed by end- diastole, whether atrial systole was present or not. Atrial systole caused partial AV valve reopening before resumption of closure.

Of special interest in the present context is that he compared AV valve closure rates for two different end-systolic volumes, while maintaining all other parameters identical. When the operating end-systolic LV volume was *small*, a *strong* " ring-vortex" (akin to a *confined* smoke-ring) formed within the chamber. The thrust of this vortex behind them initiated mid-diastolic leaflet movements toward closure, and the valve was nearly closed by end-diastole. In contrast, when the end-systolic volume was abnormally *large*, as in ventricular failure, *no* vigorous ring-vortex formed, and the valve moved sluggishly toward closure, so that it was only 25% closed at end-diastole, and reversed flow was required in order to seal it [42]. This vortical recirculation pattern and its diminished intensity with chamber enlargement are unambiguously illustrated in Fig. 4 by the intraventricular flow color mappings that were discussed above.

Bellhouse concluded that the vortex plays an important role in the normal mechanism of closure of the mitral valve, ensuring minimal regurgitation by pushing the mitral anteromedial and posterolateral leaflets toward each other prior to LV myocardial contraction [42]. However, no other plausible useful hemodynamic function had been ascertained for the diastolic vortex until the integrative diastolic function studies surveyed here and in the companion *JCTR* paper [22].

The facilitatory role of the diastolic vortex in ventricular filling

Out of these comprehensive diastolic function studies, which integrated intracardiac flow phenomena with myocardial relaxation and compliance dynamics [6,8,13,14,18,19,22], the hypothesis of a assisting role in diastolic filling was advanced for the intraventricular diastolic vortex. The key to this useful physiological role [13] of the RV and LV diastolic vortices lies in their shunting and "trapping" a certain amount of flow energy into the rotational kinetic energy of their gyratory motion, thereby preventing its Bernoulli-conversion into increased pressure with the strong flow deceleration along fanning-out streamlines (see Fig. 1, right); this becomes manifest as a decrease in the pressure energy of the inflowing blood.

This essential energy-shunting role of the filling vortex was demonstrated first in translational animal research [13], and was subsequently confirmed [7] by meticulous clinical imaging examinations using 4-D phase contrast flow MRI, a technique for assessing over time the flow velocity components in the three spatial dimensions within a flow region. By pre-empting an inflow-impeding Bernoulli pressure-rise along the fanning-out flow streamlines between AV valve anulus and the expanding endocardial surface of the chamber (see Fig. 2 and Fig. 1, right), the diastolic vortex facilitates higher diastolic filling and stroke volume maintenance. Recapitulating, the diastolic vortex shunts the inflow kinetic energy, which would otherwise contribute to the adverse convective Bernoulli pressure-rise and the

CDL, into the kinetic energy of its gyratory motion. This rotational kinetic energy is ultimately dissipated as heat [1,10,13].

The question of a role for the diastolic vortex in LV ejection

Some medical investigators [49,50] have suggested that the presence of chirally asymmetric LV diastolic vortical motions helps in the ensuing process of ejection, by conversion of vortex kinetic energy into kinetic energy of LV outflow after aortic valve opening. According to this intuitively appealing mentalistic notion, the filling vortex persisting through end-diastole would serve as a storage means for the kinetic energy of the incoming blood filling the ventricle, reducing the work necessary for the acceleration of blood into the LV outflow tract. The rotating stream of blood in the larger lobe of the persisting chirally asymmetric LV vortex would then leave the chamber in a tangential direction when ventricular contraction started. However, in dealing with fluid dynamics phenomena, intuition is treacherous.

This is an admittedly controversial topic with influential proponents on either side of the issue. It is well known in fluid mechanics that large vortices and rotational fluid flow structures *never unwind smoothly* [1,51]. Instead, as was pointed out above, they break up into smaller eddies, and this process is continued, until the vortices are reduced to micron-size eddies and at that level *(Kolmogorov "microscale")* they dissipate under the action of viscous forces [52]. The process is known as the vortical *cascade* mechanism [1]. This implies that vortices are essentially *"traps"* or *"sinks"* of energy [1,13]. Whatever kinetic energy is trapped in the recirculating motion of a vortex is bound to be converted into heat; it is bound to be lost from the motion and therefore cannot, in fact, aid ejection [1] despite the, on the face of it, intellectual appeal of a "sling-like," "morphodynamic" mode of action [49]. Vortical energy dissipation can occur both within the ventricles and within their outflow trunks and beyond.

To analyze the actual energetics of such a sling-like process, Japanese investigators [53] developed a multiscale, metaphysics heart simulation model, based on the finite element method. Taking advantage of this highly sophisticated simulation model, which encompasses electromechanical myocardial events and fluid dynamics processes, they compared the hemodynamics of ventricles with physiological and nonphysiological diastolic vortical flow paths. They examined the effects of the inflow direction in the left ventricle on its performance under conditions where other experimental variables, including ventricular morphology, myocardial properties, and pre- and afterloads, were completely matched. They found that the physiological vortical flow path did not have any energy-saving effect.

The *stroke work* performed by the LV wall was comparable at both slower and faster heart rates (physiological vortical flow path *vs.* nonphysiological, 0.864 *vs.* 0.874 *J*, at a heart rate of ≈ 60 *beats/min*; and 0.599 *vs.* 0.590 *J*, at a heart rate of ≈100 *beats/min*), indicating that vortex-associated chiral asymmetry of the flow paths in the mammalian heart has minimal, if any at all, energetic functional merit [53]. This thorough and meticulously documented investigation contradicts the notion [49,50] of an energy-saving fluidic effect of cardiac looping and chirally asymmetric LV diastolic vortical motions on ejection. Moreover, as the Japanese investigators have emphasized [53], meticulous clinical assessments [54] and outcomes of animal experiments [55,56] are in harmony with their results [1].

The atrial filling vortex

Every movement in a finite, closed space must self-evidently lead to gyration, unless a fan-like inflow pattern *transiently* leads to a *volumetrically matched* chamber expansion (cf. Fig. 1). This ensues from the law of mass conservation and the fluid's incompressibility. Thus, if

you stir coffee in a cup, rotation in some form is always generated; the usual stirring movement to mix cream is circular, but blowing into the cup toward the center produces more or less symmetric vortices, which at the surface appear akin to the pattern shown in the lower right corner of Fig. 1. It does not come as a surprise, therefore, that filling vortices have been described both in the right atrium, associated with vena caval inflow of blood [57], and in the left atrium, associated with pulmonary venous inflow [1,58,59].

Clinical implications for diastolic filling in dilated ventricles

The FI method has shown the strength of the toroidal (doughnut-shaped) ring-vortex surrounding the main inflow stream and rotating *poloidally* (in the direction of the arrow in inset c, Fig. 5) to diminish with chamber dilatation [1,8,13–17], confirming Bellhouse's ingenious mechanical models [42] demonstrating reduced diastolic vortex strength with increased chamber volume. Qualitatively, the strength of the vortex is proportional to the intensity (rotation rate) of the poloidal rotatory motion. According to its facilitatory role for ventricular inflow that was discussed above, the diastolic vortex can assist filling by eliminating CDL to a variable degree, which depends on the vortex strength [1,13,14].

In the normal-sized chamber, the strong toroidal vortex surrounding the central inflow core encroaches on the area available for flow toward the apex. This encroachment increases the central jet velocities, and causes higher linear velocities (m/s) to actually occur later—during the *downstroke* of the *E*-wave—than at peak volumetric (m^3/s) inflow rate [14], as is shown in Fig. 5. In the *enlarged* ventricles this effect is blunted, so that linear and volumetric peak velocities tend to *coincide* [14] (see Fig. 5).

These translational animal research findings are consistent with meticulous clinical results published by Yamamoto et al. [60] who compared normal intraventricular velocity patterns to those prevailing with LV enlargement, in dilated cardiomyopathy and in hypertensive heart disease. The regional diastolic velocity patterns at 1, 2, and 3 cm from the mitral tip toward the apex were recorded simultaneously with the mitral inflow velocity pattern, using multigated pulsed-Doppler. In the abnormally dilated left ventricles, linear velocities decreased strikingly from the mitral tip toward the apex [43]. In the new fluid dynamics framework for diastolic filling [1,13,14,17], this abnormal velocity distribution accrues from the diffluent (fanning-out) streamline pattern and a strong convective deceleration that in the dilated chamber persists, unabated by a strong toroidal vortex (Fig. 1, right).

In view of the integrative diastolic function framework of Fig. 1, Yamamoto et al.'s meticulous clinical findings [43] are now clearly understood to be a manifestation of the strong convective deceleration occurring as the inflow fans out—see Figs. 1 and 2—in the absence of a strong, encroaching diastolic vortex [1,8,13,14,17]. On the contrary, in subjects with normal LV function and size, the simultaneously recorded velocities at these successive sites were remarkably uniform [43]. This reflects the presence of the filling ringvortex that surrounds the central inflowing stream [13,14,17]. The strong vortex gets in the way of a fanning-out streamline pattern and prevents the ensuing strong convective deceleration from taking place—see Figs. 1, 2 and 4.

Using sophisticated digital processing of color Doppler M-mode recordings, Yotti et al., at the University Hospital Gregorio Marañón, in Madrid, Spain [61], obtained measurements of the spatiotemporal distributions of LV diastolic intraventricular pressure gradients. Their elegant findings in patients with dilated LV cardiomyopathy and their conclusions are in perfect agreement [6] with our previously published [8,13,14] fluid dynamic analyses and propositions regarding the convective deceleration load, the diastolic ventriculoannular disproportion, and the impairment of *E*-wave peak velocities and *E/A* wave ratios in dilated

ventricles. The Editorial accompanying Yotti et al.'s elegant study in *Circulation*, underscored this agreement [62].

Medical/surgical corollaries for management of RV/LV chamber dilatation

Conditions leading to eccentric hypertrophy, and remodeling with chamber enlargement as seen, e.g., in CHF or after myocardial infarction, should increase the Bernoulli-induced diastolic convective deceleration load and simultaneously reduce the intensity of the filling vortex. Both of these occurrences have been shown to contribute to the filling impairment attendant to a chamber enlargement [1,6,8,13–17]. The converse applies for surgical interventions, such as the Batista procedure (partial left ventriculectomy), and medical treatments attenuating or reversing pathological ventricular remodeling and chamber enlargement [1,11]. Medical interventions include cardiac resynchronization therapy (atrial-synchronized biventricular pacing) to reverse the remodeling seen in CHF and improve cardiac structure and function [42,63,64], and the attenuation of ventricular remodeling and LV operating volume elevations after myocardial infarction by the administration of cell therapy or ACE inhibitors [65]. Such interventions should act, in part, by decreasing ESV (see discussion in subsection "Diastolic ventriculoannular disproportion and clinical indicators of elevated CDL") and, thus, the diastolic CDL, and by diminishing the diastolic ventriculoannular disproportion [14,17] as well as promoting stronger diastolic vortices within the less-dilated chambers [13].

Conversely, diastolic ventriculoannular disproportion and the convective deceleration load should be augmented by a cardiac procedure-associated pericardiotomy when chamber dilatation is no longer curtailed by pericardial restraint, as in cases of *acute* or *subacute* systolic LV dysfunction, before gradual compensatory pericardial expansion that ensues with chronic cardiac enlargement [22]. More importantly, DVAD with augmentation of CDL occurs initially after surgical interventions, i.e., tricuspid or mitral ring annuloplasties, which decrease the effective tricuspid or mitral orifice cross-section relative to RV or LV chamber volume and inner surface area [66]. However, the subsequent regression of abnormal remodeling—reversal of chamber dilatation and eventual chamber-size normalization—remedies this transitory situation. Such considerations point toward innovative translational research directions.

Fluid dynamic interactions of systolic and diastolic dysfunction

In primary systolic dysfunction and failure, impaired contractile performance is the principal functional derangement; it is the major mechanism for the right and downward shift of the end-systolic pressure–volume line (see Fig. 6, lower right) and the diminished ejection fraction. Increased passive stiffness and impaired ventricular relaxation are the traditionally recognized [2,22] functional derangements in primary diastolic dysfunction and failure. The diastolic pressure-volume relation shifts upward and to the left (Fig. 6, lower left); consequently, there is a disproportionately large diastolic pressure increase as volume rises during diastolic filling, leading to raised atrial and upstream venous pressures.

In primary systolic dysfunction and failure, ensuing diastolic dysfunction as gauged by a ventricular filling impairment is common, particularly with a substantially raised end-systolic ventricular volume (see Fig. 6, top). In the innovative framework surveyed here [1,6,8,13–15,17], the increased end-systolic/early-diastolic chamber size induces ventriculoannular disproportion with a disproportionate increase of the CDL and a *weakening* of the filling vortex that normally facilitates filling by impounding inflow kinetic energy and averting an inflow-impeding, convective Bernoulli pressure-rise [13]; elevated intraventricular diastolic filling pressure levels ensue (Fig. 6, lower left). More difficult ventricular diastolic inflow and filling impairment can accrue from these changes. This

sequence of events explains the intriguing observation (alluded to in the Introduction) that *diastolic* function is frequently abnormal in patients with primary *systolic* dysfunction and failure.

The new framework complements conventional assessments of diastolic function in failure and remodeling, by encompassing heretofore overlooked vital fluid dynamics aspects. Thus (Fig. 6, top), through the increased end-systolic ventricular volume and CDL, with diminished vortex strength and superimposed filling impairment, an underlying *systolic* dysfunction and failure can beget *diastolic* dysfunction. Conversely, *diastolic* dysfunction with impaired chamber filling in absence of effective "atrial kick" compensation (e.g., in atrial fibrillation) can lead directly to a preload-dependent stroke volume *curtailment*: the stroke volume decline accrues from decreased EDV, while systolic myocardial function and contractility may remain normal.

Epigenetic propositions and directions for functional genomics research

Epigenetics affects the interpretation of DNA genetic sequences in cells; they help drive cell processes by regulating when and how genes are activated. The epigenome [67] is an important target of "environmental" forces. One way in which DNA expression can be controlled in response to such forces is by the methylation (addition of a bulky methyl group) to one of the DNA bases [67,68,69], rendering this "tagged" area of the DNA less active and perhaps suppressing the production of a particular protein. Methylation modifies only the C (cytosine) of the four-letter DNA "alphabet" (A, G, C and T). The abnormal methylation of genes can ultimately lead to alterations of normal cardiomyocyte functions and to the development of heart disease. Another way that gene expression can be modified involves the histones, the chief protein components of chromatin, which act as spools around which DNA winds. Histone proteins are subject to a variety of modifications, the combination of which creates a code (histone code) that influences the gene transcriptional status and the expression of genetic information, by modulating the chromatin structure and DNA accessibility [67,70,71,72,73].

Epigenetic mechanisms acting as switches in gene expression in response to various stimuli are fundamental in cardiac adaptations, remodeling, reverse remodeling, and disease. They underlie "phenotypic plasticity" (or "plastic adaptation") and can lead the *same* combination of genes to produce *different* structural/functional outcomes, depending on "environmental" variation or stimuli [74,75] to which they are exposed; i.e. the environment can have a direct impact on the phenotype without any genetic change [76].

In a contemporaneous survey [77], I propose that changing "environmental" forces associated with diastolic RV and LV rotatory flows during filling exert important, albeit still unappreciated, epigenetic actions influencing functional and morphological cardiac adaptations. Mechanisms analogous to Murray's law of hydrodynamic shear-induced endothelial cell modulation of vascular geometry are likely to link to RV/LV adaptations [1,77] the variable laminar vortical shear and centrifugal "squeeze" forces, which are exerted by the poloidally rotating blood (cf. inset c, Fig. 5) on the endocardium and myocardial walls. By Newton's Third Law, the centrifugal force is directed away from the center of vortical rotation and is exerted *by* the revolving blood *on* the ventricular walls that provide its centripetal acceleration—see Fig. 7.

The time has come to explore a new paradigm in which intraventricular diastolic filling vortex-associated forces play a fundamental epigenetic role, and to work out how heart cells react to these forces and to changes in their intensity [77], connected to ventricular chamber enlargement and remodeling of manifold etiologies. In this context, the epigenome can be interpreted as a template placed over the potential blueprint of the genome, with variously

positioned openings depending on the phenotype that is to arise in a given "environment." *Exposed* are the blueprint genes that are actually expressed, whereas *covered* are genes that are not expressed.

In future research, ventricular tissue samples from dilated ventricles having reduced vortex strength can be compared against samples from control ventricles having diastolic filling vortices of normal strength. The myocardial samples can be individually analyzed for DNA methylation/histone modifications and expressional changes using expression microarrays and gene promoter microarrays to identify differentially methylated gene promoters between the 2 groups [78,79,80,81].

Elucidating the role of epigenetic mechanisms in ventricular dilatation and failure could provide a basis for the development of new therapeutic approaches to ventricular dilatation and failure associated with diminished vortex strength and ventricular filling [77]; appropriate modulation of epigenetic structure could *correct* gene expression. This new frontier in contemporary cardiac research should uncover versatile mechanistic insights linking filling vortex patterns and attendant forces to variable expressions of gene regulation in RV/LV myocardium. In due course, it should reveal intrinsic homeostatic arrangements that support ventricular myocardial function and adaptability, and their disturbances. Such advances should lead to improved (patho) physiologic understanding and to innovative and more effective treatments of heart failure-related structural and functional remodeling and of ventricular dilatation of diverse origins. Indeed, appropriate modulation of epigenetic structure could correct gene expression of myocardial cells impacted by abnormal diastolic vortex dynamics. As Dr. Victor Dzau, currently Chancellor of Health Affairs at Duke has summed up in an Editorial [82], Dr. Daniel Tosteson of Harvard arrived more than 15 years ago at the astute conclusion that: "In the past we have had functions in search of sequences. In the future, pathology and physiology will become *functionators* for the sequences." It rings so tantalizing true today for those engaged in cardiac translational research!

Conclusions

This article has summarized concepts regarding normal diastolic function and its disturbances in ventricular dilatation from multiple etiologies, including primary systolic dysfunction and heart failure, with central emphasis on developing a useful innovative framework for approaching ventricular filling dynamics in RV/LV failure. In the setting of ventricular chamber enlargement, fundamental cardiac fluid dynamic mechanisms can impair diastolic filling even in the absence of inflow valvular stenosis or of abnormalities of myocardial relaxation and ventricular diastolic compliance.

The diastolic vortex facilitates filling. The CDL is an important determinant of RV or LV inflow during the *E*-wave (*A*-wave) upstroke. The larger the chamber, the larger the CDL; its magnitude affects strongly peak *E*- (and *A*-wave) velocities. This underlies the concept of diastolic ventriculoannular disproportion. Large-scale vortical motions after the *E*-wave peak impound inflow kinetic energy, preventing an inflow-impeding Bernoulli pressure-rise between inflow orifice and the expanding endocardial surface. This reduces the CDL by a variable amount, depending on vortical intensity, which decreases with chamber dilatation.

The new framework complements myocardial and ventricular mechanics [2,22] assessments of diastolic dysfunction in failure/remodeling, by encompassing heretofore overlooked but vital dynamic aspects of diastolic intraventricular flow. It also provides stimulus for functional genomics research, which promises to rapidly narrow the gap between gene sequence and myocardial function and to yield new insights into ventricular adaptive and maladaptive remodeling.

Summing up, irrespective of any other possible coexisting myocardial and ventricular abnormalities, chamber enlargement—a hallmark of ventricular systolic dysfunction and failure— in and by itself impairs diastolic filling, by enhancing the convective deceleration load and by diminishing the strength of the inflow-facilitating, beneficial diastolic intraventricular vortex. Contemporary cardiac research should uncover versatile mechanistic insights linking filling vortex patterns and attendant forces to variable expressions of myocardial gene regulation.

Acknowledgments

Research support, for work in the author's Laboratory surveyed in this Review, was provided by the National Heart, Lung, and Blood Institute [grant number R01-HL- 050446]; the National Science Foundation [grant number CDR 8622201]; and the North Carolina Supercomputing Center and Cray Research. I thank the co-Editor-in-Chief and the reviewers for their constructive remarks. The final product has benefited greatly from Dr. Hall's interest and personal editorial attention.

References

1. Pasipoularides, A. Heart's vortex: intracardiac blood flow phenomena. Shelton: People's Medical Publishing House; 2010. p. 960
2. Mirsky I, Pasipoularides A. Clinical assessment of diastolic function. Prog Cardiovasc Dis. 1990; 32:291–318. [PubMed: 2405455]
3. Zile MR, Baicu CF, Gaasch WH. Diastolic heart failure: abnormalities in active relaxation and passive stiffness of the left ventricle. N Engl J Med. 2004; 350:1953–1959. [PubMed: 15128895]
4. Kass DA, Bronzwaer JG, Paulus WJ. What mechanisms underlie diastolic dysfunction in heart failure? Circ Res. 2004; 94:1533–1542. [PubMed: 15217918]
5. Pasipoularides A. Clinical assessment of ventricular ejection dynamics with and without outflow obstruction. [Review]. J Am Coll Cardiol. 1990; 15:859–882. [PubMed: 2407763]
6. Pasipoularides, A. Right and left ventricular diastolic flow field: why are measured intraventricular pressure gradients small? [Flujo diastólico ventricular derecho e izquierdo: ¿por qué son bajos los gradientes de presión intraventricular medidos?]. Rev Esp Cardiol. 2012. [In press] http://dx.doi.org/10.1016/j.recesp.2012.07.019
7. Fredriksson AG, Zajac J, Eriksson J, Dyverfeldt P, Bolger AF, Ebbers T, Carlhäll CJ. 4-D blood flow in the human right ventricle. Am J Physiol Heart Circ Physiol. 2011; 301:H2344–H2350. [PubMed: 21926347]
8. Pasipoularides A, Shu M, Womack MS, Shah A, von Ramm O, Glower DD. RV functional imaging: 3-D Echo-derived dynamic geometry and flow field simulations. Am J Physiol Heart Circ Physiol. 2003; 284:H56–H65. [PubMed: 12388220]
9. Borlaug BA, Redfield MM. Diastolic and systolic heart failure are distinct phenotypes within the heart failure spectrum. Circulation. 2011; 123:2006–2013. [PubMed: 21555723]
10. Pasipoularides A. LV twisting-and-untwisting in HCM: ejection begets filling. Diastolic functional aspects of HCM. [Progress in Cardiology]. Am Heart J. 2011; 162:798–810. [PubMed: 22093194]
11. Tønnessen T, Knudsen CW. Surgical left ventricular remodelling in heart failure. Eur J Heart Fail. 2005; 7:704–709. [PubMed: 16087128]
12. Isaaz K, Pasipoularides A. Noninvasive assessment of intrinsic ventricular load dynamics in dilated cardiomyopathy. J Am Coll Cardiol. 1991; 17:112–121. [PubMed: 1987212]
13. Pasipoularides A, Shu M, Shah A, Womack MS, Glower DD. Diastolic right ventricular filling vortex in normal and volume overload states. Am J Physiol Heart Circ Physiol. 2003; 284:H1064–H1072. [PubMed: 12666664]
14. Pasipoularides A, Shu M, Shah A, Tucconi A, Glower DD. RV instantaneous intraventricular diastolic pressure and velocity distributions in normal and volume overload awake dog disease models. Am J Physiol Heart Circ Physiol. 2003; 285:H1956–H1968. [PubMed: 14561678]

15. Pasipoularides A. Complementarity and competitiveness of the intrinsic and extrinsic components of the total ventricular load: Demonstration after valve replacement in aortic stenosis [Editorial]. Am Heart J. 2007; 153:4–6. [PubMed: 17174626]

16. Pasipoularides A. Invited commentary: Functional Imaging (FI) combines imaging datasets and computational fluid dynamics to simulate cardiac flows. J Appl Physiol. 2008; 105:1015. [PubMed: 18800398]

17. Pasipoularides, A. Analysis of vortex flow imaging in normal and dysfunctional RV's. PROLibraries.com; American Society of Echocardiography 22nd Annual Scientific Sessions, Montreal, EE02d - Flow Vortex Imaging; 2011. http://www.prolibraries.com/ase/?select=session&sessionID=3049

18. Pasipoularides AD, Shu M, Shah A, Glower DD. Right ventricular diastolic relaxation in conscious dog models of pressure overload, volume overload and ischemia. J Thorac Cardiovasc Surg. 2002; 124:964–972. [PubMed: 12407380]

19. Pasipoularides AD, Shu M, Shah A, Silvestry S, Glower DD. Right ventricular diastolic function in canine models of pressure overload, volume overload and ischemia. Am J Physiol Heart Circ Physiol. 2002; 283:H2140–H2150. [PubMed: 12384492]

20. Ihara T, Shannon RP, Komamura K, Pasipoularides A, Patrick T, Shen YT, Vatner SF. Effects of anesthesia and recent surgery on diastolic function. Cardiovasc Res. 1994; 28:325–336. [PubMed: 8174152]

21. Condos WRJ, Latham RD, Hoadley SD, Pasipoularides A. Hemodynamics of the Mueller maneuver in man: right and left heart micromanometry and Doppler echocardiography. Circulation. 1987; 76:1020–1028. [PubMed: 3664990]

22. Pasipoularides A. Right and left ventricular diastolic pressure-volume relations: a comprehensive review. J Cardiovasc Transl Res. 2013; 6:239–252. [PubMed: 23179133]

23. Craig, WE.; Murgo, JP.; Pasipoularides, A. Calculation of the time constant of relaxation. In: Grossman, W.; Lorell, B., editors. Diastolic relaxation of the heart. The Hague: Martinus Nijhoff; 1987. p. 125-132.

24. Zile MR, Tomita M, Ishihara K, Nakano K, Lindroth J, Spinale F, Swindle M, Carabello BA. Changes in diastolic function LV volume overload produced by mitral regurgitation. Circulation. 1993; 87:1378–1388. [PubMed: 8462159]

25. Pacileo G, Limongelli G, Verrengia M, Gimeno J, Di Salvo G, Calabrò R. Backscatter evaluation of myocardial functional and textural findings in children with right ventricular pressure and/or volume overload. Am J Cardiol. 2004; 93:594–597. [PubMed: 14996585]

26. Wang XF, Deng YB, Nanda NC, Deng J, Miller AR, Xie MX. Live three-dimensional echocardiography: imaging principles and clinical application. Echocardiography. 2003; 20:593–604. [PubMed: 14536007]

27. Bazilevs Y, del Alamo JC, Humphrey JD. From imaging to prediction: emerging noninvasive methods in pediatric cardiology. Prog Ped Cardiol. 2010; 30:81–89.

28. Ebbers T, Wigstrom L, Bolger AF, Engvall J, Karlsson M. Estimation of relative cardiovascular pressures using time-resolved three-dimensional phase contrast MRI. Magn Reson Med. 2001; 45:872–879. [PubMed: 11323814]

29. Bolger AF, Heiberg E, Karlsson M, Wigström L, Engvall J, Sigfridsson A, Ebbers T, Kvitting JP, Carlhäll CJ, Wranne B. Transit of blood flow through the human left ventricle mapped by cardiovascular magnetic resonance. J Cardiovasc Magn Reson. 2007; 9:741–747. [PubMed: 17891610]

30. Lu J, Li W, Zhong Y, Luo A, Xie S, Yin L. Intuitive visualization and quantification of intraventricular convection in acute ischemic left ventricular failure during early diastole using color Doppler-based echocardiographic vector flow mapping. Int J Cardiovasc Imaging. 2012; 28:1035–1047. [PubMed: 21814809]

31. Mangual J, Domenichini F, Pedrizzetti G. Describing the highly 3D flow in the right ventricle. Ann Biomed Eng. 2012; 40:1790–1801. [PubMed: 22396043]

32. Inwood, S. The Forgotten Genius: The Biography of Robert Hooke 1635–1703. San Fransisco: MacAdam/Cage; 2003. p. 105

33. Pasipoularides A, Murgo JP, Miller JW, Craig WE. Nonobstructive left ventricular ejection pressure gradients in man. Circ Res. 1987; 61:220–227. [PubMed: 3621488]
34. Bird JJ, Murgo JP, Pasipoularides A. Fluid dynamics of aortic stenosis: subvalvular gradients without subvalvular obstruction. Circulation. 1982; 66:835–840. [PubMed: 6889475]
35. Pasipoularides A, Murgo JP, Bird JJ, Craig WE. Fluid dynamics of aortic stenosis: Mechanisms for the presence of subvalvular pressure gradients. Am J Physiol. 1984; 246:H542–H550. [PubMed: 6720911]
36. Georgiadis JG, Wang M, Pasipoularides A. Computational fluid dynamics of left ventricular ejection. Ann Biomed Eng. 1992; 20:81–97. [PubMed: 1562106]
37. Pasipoularides A. Fluid dynamic aspects of ejection in hypertrophic cardiomyopathy. [Review]. Hellenic J Cardiol. 2011; 52:416–426. [PubMed: 21940289]
38. Isaaz K. Expanding the frontiers of Doppler echocardiography for the noninvasive assessment of diastolic hemodynamics. J Am Coll Cardiol. 2000; 36:1950–1952. [PubMed: 11092669]
39. Houlind K, Schroeder AP, Egeblad H, Pedersen EM. Age-dependent changes in spatial and temporal blood velocity distribution of early left ventricular filling. Magn Reson Imaging. 1999; 17:859–868. [PubMed: 10402593]
40. Cortina C, Bermejo J, Yotti R, Desco MM, Rodríguez-Pérez D, Antoranz JC, Rojo-Alvarez JL, Garcia D, Garcia-Fernandez MA, Fernandez-Aviles F. Noninvasive assessment of the right ventricular filling pressure gradient. Circulation. 2007; 116:1015–1023. [PubMed: 17684149]
41. Yu CM, Sanderson JE, Gorcsan J 3rd. Echocardiography, dyssynchrony, and the response to cardiac resynchronization therapy. Eur Heart J. 2010; 31:2326–2337. [PubMed: 20709721]
42. Yu CM, Fung WH, Lin H, Zhang Q, Sanderson JE, Lau CP. Predictors of left ventricular reverse remodeling after cardiac resynchronization therapy for heart failure secondary to idiopathic dilated or ischemic cardiomyopathy. Am J Cardiol. 2003; 91:684–688. [PubMed: 12633798]
43. Khaykin Y, Exner D, Birnie D, Sapp J, Aggarwal S, Sambelashvili A. Adjusting the timing of left-ventricular pacing using electrocardiogram and device electrograms. Europace. 2011; 13:1464–1470. [PubMed: 21596719]
44. Taylor DEM, Wade JD. Pattern of blood flow within the heart: a stable system. Cardiovasc Res. 1973; 7:14–21. [PubMed: 4694955]
45. Rodevand O, Bjornerheim R, Edvardsen T, Smiseth OA, Ihlen H. Diastolic flow pattern in the normal left ventricle. J Am Soc Echocardiogr. 1999; 12:500–507. [PubMed: 10359922]
46. Alhama M, Bermejo J, Yotti R, Perez-David E, Benito Y, Gonzalez-Mansilla A, Perez del Villar C, Fernandez-Aviles F, del Alamo J. Quantitative assessment of intraventricular vorticity using conventional color-Doppler ultrasound. Head to head clinical validation against phase-contrast magnetic resonance imaging. J Am Coll Cardiol. 2012; 59(13s1):E1128–E1128.
47. Benito Y, Bermejo J, Alhama M, Yotti R, Perez del Villar C, Martínez-Legazpi P, Gonzalez-Mansilla A, Barrio A, Fernandez-Aviles F, del Alamo JC. Heart rate and AV delay modify left ventricular filling vortex properties. Circulation. 2012; 126:A18099.
48. Bellhouse BJ. Fluid mechanics of a model mitral valve and left ventricle. Cardiovasc Res. 1972; 6:199–210. [PubMed: 5034234]
49. Kilner PJ, Yang GZ, Wilkes AJ, Mohiaddin RH, Firmin DN, Yacoub MH. Asymmetric redirection of flow through the heart. Nature. 2000; 404:759–761. [PubMed: 10783888]
50. Taylor TW, Yamaguchi T. Flow patterns in three-dimensional left ventricular systolic and diastolic flows determined from computational fluid dynamics. Biorheology. 1995; 32:61–71. [PubMed: 7548861]
51. She ZS, Waymire EC. Quantized energy cascade and Log-Poisson statistics in fully developed turbulence. Phys Rev Lett. 1995; 74:262–265. [PubMed: 10058344]
52. She ZS, Waymire EC. Quantized energy cascade and Log-Poisson statistics in fully developed turbulence. Phys Rev Lett. 1995; 74:262–265. [PubMed: 10058344]
53. Watanabe H, Sugiura S, Hisada T. The looped heart does not save energy by maintaining the momentum of blood flowing in the ventricle. Am J Physiol Heart Circ Physiol. 2008; 294:H2191–H2196. [PubMed: 18326797]

54. Maire R, Ikram S, Odemuyiwa O, Groves PH, Lo SV, Banning AP, Hall RJ. Abnormalities of left ventricular flow following mitral valve replacement: a colour flow Doppler study. Eur Heart J. 1994; 15:293–302. [PubMed: 8013500]

55. Elbeery JR, Lucke JC, Feneley MP, Maier GW, Owen CH, Savitt MA, Gall SAJ, Glower DD, Van Trigt P, Rankin JS. The mechanical determinants of myocardial oxygen consumption in the conscious dog. Am J Physiol Heart Circ Physiol. 1995; 269:H609–H620.

56. Glower DD, Spratt JA, Snow ND, Kabas JS, Davis JW, Olsen CO, Tyson GS, Sabiston DCJ, Rankin JS. Linearity of the Frank-Starling relationship in the intact heart: the concept of preload recruitable stroke work. Circulation. 1985; 71:994–1009. [PubMed: 3986986]

57. Rushmer, RF. Cardiovascular Dynamics. 3. Philadelphia, London, Toronto: W. B. Saunders Co; 1970. p. 50

58. Fyrenius A, Wigström L, Ebbers T, Karlsson M, Engvall J, Bolger AF. Three dimensional flow in the human left atrium. Heart. 2001; 86:448–455. [PubMed: 11559688]

59. Park KH, Son JW, Park WJ, Lee SH, Kim U, Park JS, Shin DG, Kim YJ, Choi JH, Houle H, Vannan MA, Hong GR. Characterization of the left atrial vortex flow by two-dimensional transesophageal contrast echocardiography using particle image velocimetry. Ultrasound Med Biol. 2013; 39:62–71. [PubMed: 23079000]

60. Yamamoto K, Masuyama T, Tanouchi J, Naito J, Mano T, Kondo H, Nagano R, Hori M, Kamada T. Intraventricular dispersion of early diastolic filling: a new marker of left ventricular diastolic dysfunction. Am Heart J. 1995; 129:291–299. [PubMed: 7832102]

61. Yotti R, Bermejo J, Antoranz JC, Desco MM, Cortina C, Rojo-Alvarez JL, Allué C, Martín L, Moreno M, Serrano JA, Muñoz R, García-Fernández MA. A noninvasive method for assessing impaired diastolic suction in patients with dilated cardiomyopathy. Circulation. 2005; 112:2921–2929. [PubMed: 16275881]

62. Little WC. Diastolic dysfunction beyond distensibility; adverse effects of ventricular dilatation. Circulation. 2005; 112:2888–2890. [PubMed: 16275877]

63. Abraham WT, Hayes DL. Cardiac resynchronization therapy for heart failure. Circulation. 2003; 108:2596–2603. [PubMed: 14638522]

64. St John Sutton M, Ghio S, Plappert T, Tavazzi L, Scelsi L, Daubert C, Abraham WT, Gold MR, Hassager C, Herre JM, Linde C. REsynchronization reVErses Remodeling in Systolic left vEntricular dysfunction (REVERSE) Study Group. Cardiac resynchronization induces major structural and functional reverse remodeling in patients with New York Heart Association class I/II heart failure. Circulation. 2009; 120:1858–1865. [PubMed: 19858419]

65. Sutton MG, Sharpe N. Left ventricular remodeling after myocardial infarction: pathophysiology and therapy. Circulation. 2000; 101:2981–2988. [PubMed: 10869273]

66. Glower DD, Tuttle RH, Shaw LK, Orozco RE, Rankin JS. Patient survival characteristics after routine mitral valve repair for ischemic mitral regurgitation. J Thorac Cardiovasc Surg. 2005; 129:860–868. [PubMed: 15821655]

67. Bernstein BE, Meissner A, Lander ES. The mammalian epigenome. Cell. 2007; 128:669–681. [PubMed: 17320505]

68. Klose RJ, Bird AP. Genomic DNA methylation: the mark and its mediators. Trends Biochem Sci. 2006; 31:89–97. [PubMed: 16403636]

69. Weber M, Schübeler D. Genomic patterns of DNA methylation: targets and function of an epigenetic mark. Curr Opin Cell Biol. 2007; 19:273–280. [PubMed: 17466503]

70. Kouzarides T. Chromatin modifications and their function. Cell. 2007; 128:693–705. [PubMed: 17320507]

71. Chang CP, Bruneau BG. Epigenetics and cardiovascular development. Annual review of physiology. 2012; 74:41–68.

72. Rusk N. Writing the histone code. Nat Methods. 9:777. [PubMed: 23019686]

73. Lorenzen JM, Martino F, Thum T. Epigenetic modifications in cardiovascular disease. Basic Res Cardiol. 2012; 107:245.10.1007/s00395-012-0245-9 [PubMed: 22234702]

74. Sollars V, Lu X, Xiao L, Wang X, Garfinkel MD, Ruden DM. Evidence for an epigenetic mechanism by which Hsp90 acts as a capacitor for morphological evolution. Nat Genet. 2003; 33:70–74. [PubMed: 12483213]

75. Feinberg AP. Phenotypic plasticity and the epigenetics of human disease. Nature. 2007; 447:433–440. [PubMed: 17522677]

76. Réale D, McAdam AG, Boutin S, Berteaux D. Genetic and plastic responses of a northern mammal to climate change. Proc R Soc Lond B. 2003; 270:591–596.

77. Pasipoularides A. Diastolic filling vortex forces and cardiac adaptations: probing the epigenetic nexus. Hellenic J Cardiol. 2012; 53:458–469. [PubMed: 23178429]

78. Dahl C, Guldberg P. DNA methylation analysis techniques. Biogerontology. 2003; 4:233–250. [PubMed: 14501188]

79. Koga Y, Pelizzola M, Cheng E, Krauthammer M, Sznol M, Ariyan S, Narayan D, Molinaro AM, Halaban R, Weissman SM. Genome-wide screen of promoter methylation identifies novel markers in melanoma. Genome Res. 2009; 19:1462–1470. [PubMed: 19491193]

80. Lee EK. Large-scale optimization-based classification models in medicine and biology. Ann Biomed Eng. 2007; 35:1095–1109. [PubMed: 17503186]

81. Huang da W, Sherman BT, Lempicki RA. Systematic and integrative analysis of large gene lists using DAVID bioinformatics resources. Nature protocols. 2009; 4:44–57.

82. Dzau VJ, Austin MJ, Brown P, Cowley A, Housman D, Mulligan R, Rosenberg R. Revolution and renaissance. Physiol Genomics. 1999; 1:1–2. [PubMed: 11015554]

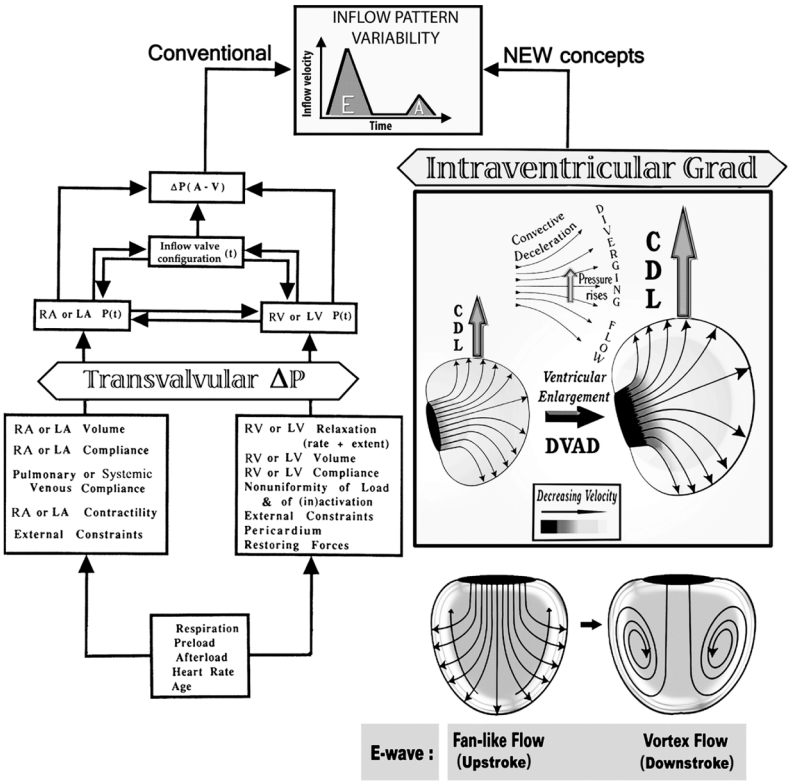

Fig. 1.

The determinants of ventricular inflow patterns and diastolic filling include factors intrinsic and extrinsic to the right and left ventricles. The new diastolic function paradigm (right panels) complements and acts in parallel with the traditional one (left): changes in RV/LV size, diastolic myocardial dynamics, and wall motion patterns cause concomitant alterations in the magnitude of the convective deceleration load (CDL) and the properties of the diastolic vortex, which affect inflow patterns and ventricular filling. A=atrial; V=ventricular; P=pressure; t=time; DVAD=diastolic ventriculoannular disproportion; Grad=P gradient. (Adapted from Pasipoularides [1], by permission of PMPH-USA.)

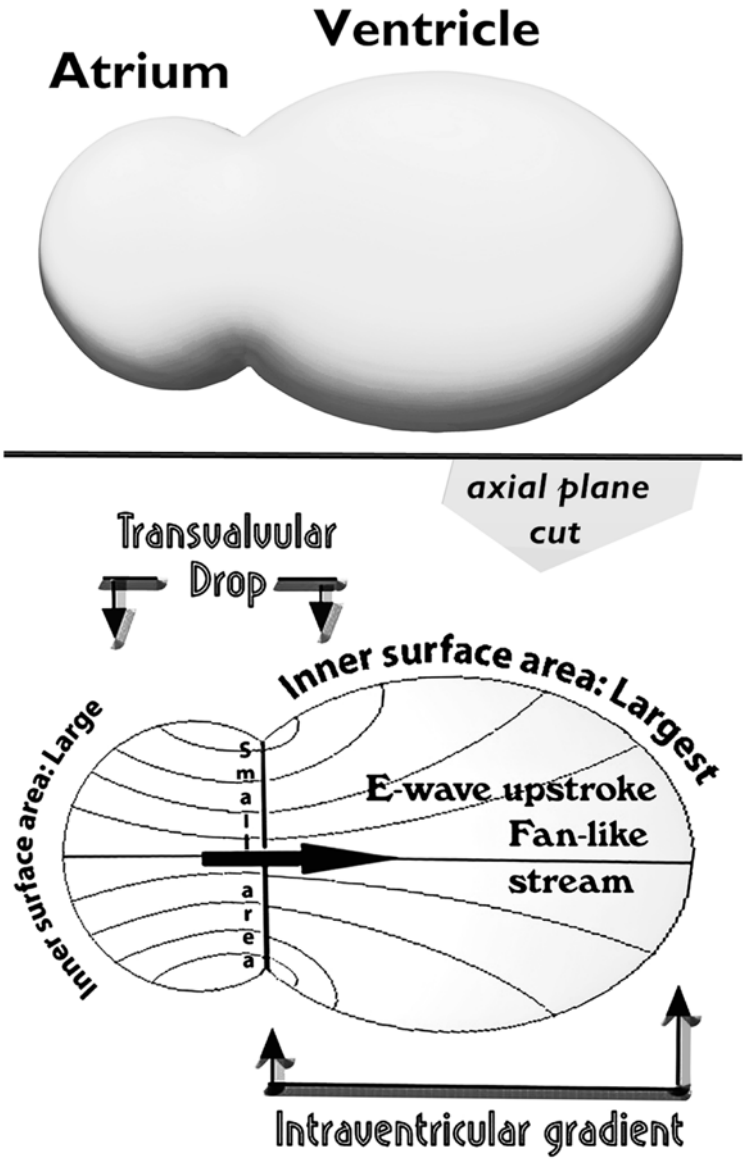

Fig. 2.

During the *E*-wave upstroke, flow is confluent between atrial endocardium and atrioventricular valve orifice and diffluent between the latter and the ventricular chamber walls. There is convective acceleration up to the orifice and convective *deceleration* beyond it. Transvalvular pressure drops embody convective acceleration, whereas intraventricular gradients convective deceleration, which counterbalances in part the simultaneous local acceleration gradient during the *E*-wave upstroke. These convective pressure gradients are much greater (depend on r^2, where r is an effective radial coordinate) in 3-D space than what might be anticipated on the basis of 2-D projections (dependence on r).

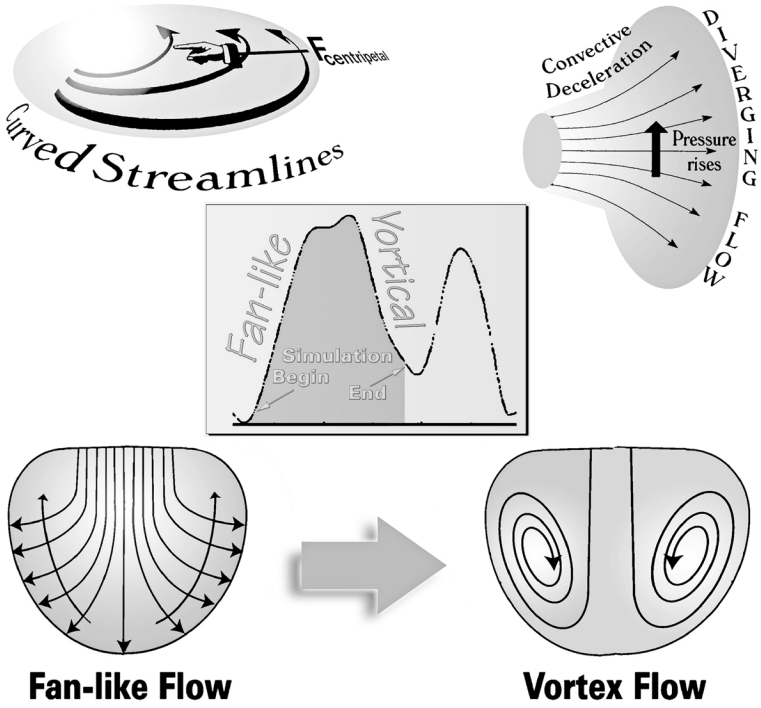

Fig. 3.

As blood fans away from the central stream toward the endocardial walls, the convective deceleration effect tends, by the Bernoulli mechanism, to elevate downstream pressure opposing ventricular inflow (*top right*). There is an additional convective pressure decrease normal to the curved fanning streamlines (*top left*), which tends to decrease pressure in the direction of the chamber's base and away from the endocardial walls (long arrows crossing streamlines, *lower left*). During the upstroke of the *E*-wave, these combined adverse convective pressure effects are opposed by the local acceleration gradient, which favors forward flow. During the *E*-wave downstroke, they are joined in sense and augmented by the local deceleration gradient and can now reverse the flow. This leads to disruption of the boundary between oncoming blood and endocardial walls, or "flow separation," and to the formation of a toroidal vortex that surrounds the central core (*lower right*). *Center inset*: volumetric filling rate calculated by numerical differentiation of RV chamber volume obtained from dynamic representations using combined real-time 3-D echocardiographic and sonomicrometric measurements; small arrows point to representative beginning and ending points of the FI simulations. (Adapted, somewhat modified, from Pasipoularides [1], by permission of PMPH-USA.)

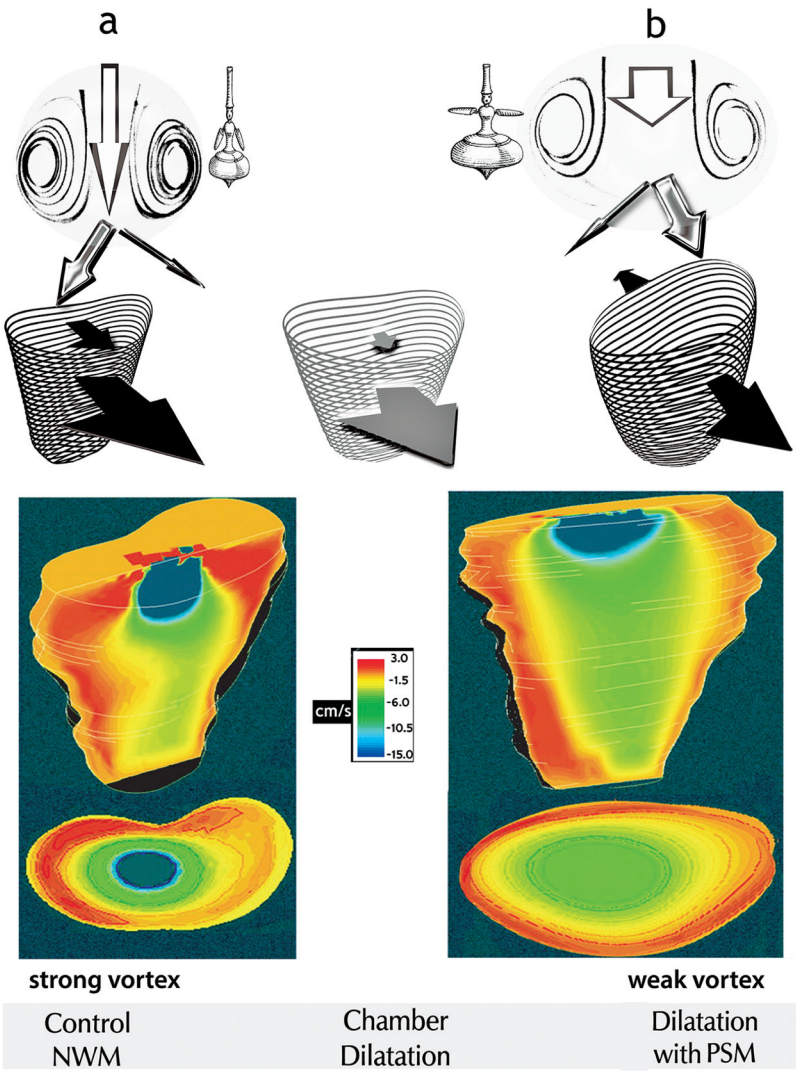

Fig. 4.

Top panels Under control conditions with normal wall motion (NWM), diastolic filling entails anterior-directed motion of both the free RV wall and the septum (black arrows, a). In RV chamber dilatation with paradoxical septal motion (PSM), the septum moves toward the left ventricle (back-pointing black arrow, b). Interposed is the pattern of RV dilatation with normal septal motion (gray arrows). By increasing both intraventricular mass and effective rotation radii, increased chamber size yields smaller recirculating velocities and vortex strength, as the "whirling dervish" tops suggest: with arms extended and wider girth, spinning is slower in b than in a. The stronger vortex ring in the normal-sized chamber (panels a) encroaches more on the central core than the weaker vortex in the enlarged chamber (panels b). Consequently, although instantaneous volumetric inflow rates at control were smaller than with volume overload, after vortex development higher linear core velocities were present at control than with chamber dilatation attendant to volume overload. The width of each white arrow in the top panels is proportional to central core area; the length, to linear inflow velocity.

Bottom panels: Simultaneous frontal-plane and transverse (at a level 2.5 *cm* below the inflow orifice) sections showing RV color flow maps, close to the end of the *E*-wave. The instantaneous volumetric inflow velocities were 39 cm^3/s in the normal-sized (*left*) and 71

cm^3/s in the dilated (*right*) chamber, respectively. These Functional Imaging mappings show expediently the higher axial core velocities in the normal and the larger core cross-section in the enlarged chamber. (Color maps reproduced from Pasipoularides et al. [13] by permission of The American Physiological Society.)

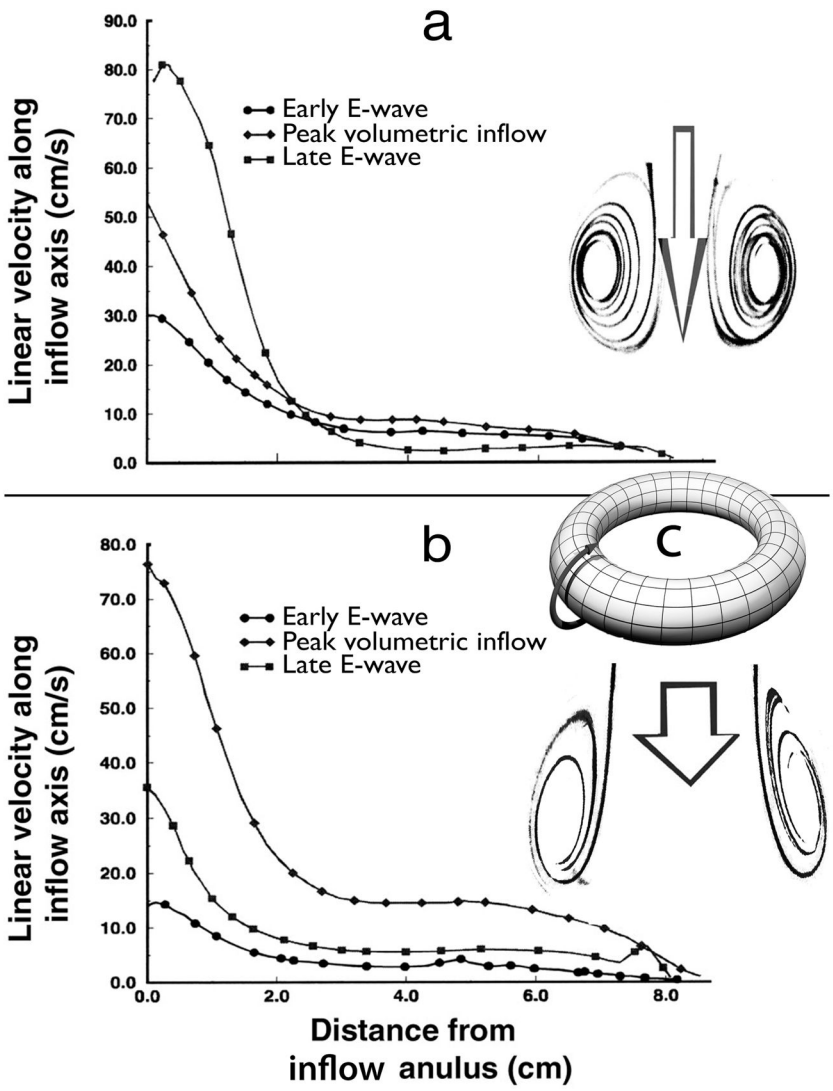

Fig. 5.

Velocity distributions along the RV inflow axis from Functional Imaging simulations: a, at control; b, with chamber enlargement. At control, although the volumetric inflow rate is then much lower, inflow velocities along the axis in the basal region of the chamber are substantially higher *late* in the *E*-wave than their levels at the peak volumetric inflow rate, E_{pk}. This unexpected phenomenon is a corollary of the intense squeeze of the inflow core at control by the encircling strong ring-vortex, as hinted by the graphic insets accompanying the velocity distribution plots. Arrow length is proportional to linear velocity; arrow width, to volumetric inflow rate. Inset c depicts schematically the ring-vortex surrounding the inflowing core-stream and rotating *poloidally, i.e.,* in the sense of the curved arrow. This poloidal rotation pattern is akin to that of the magnetic field in a magnet, which flows from the north pole to the south pole; hence, the name. (Reproduced, slightly modified, from Pasipoularides et al. [14] by permission of The American Physiological Society.)

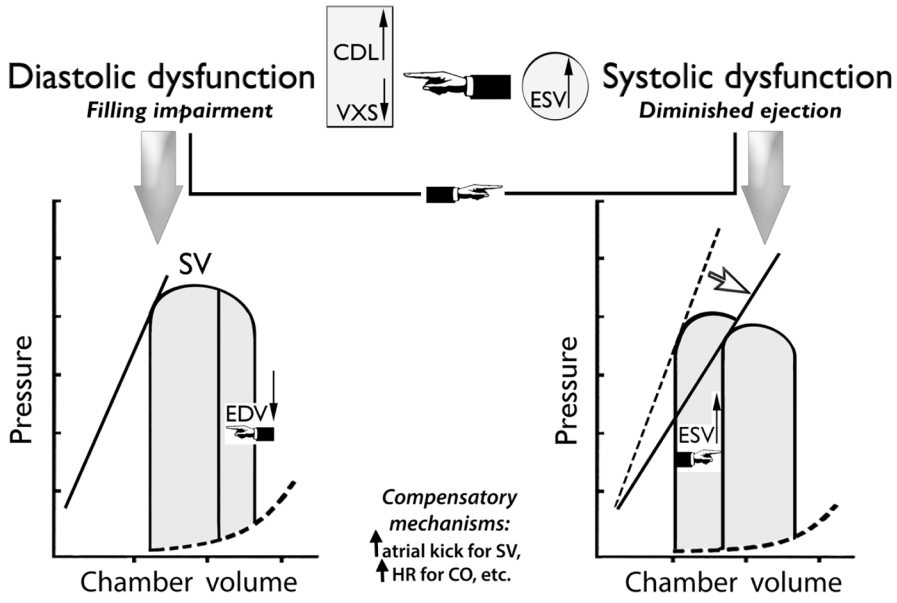

Fig. 6.

Bottom panels in diastolic dysfunction/failure, the diastolic pressure-volume relation (dashed curve) shifts upward-and-leftward (counter-clockwise rotation), indicative of disproportionately large pressure increments as volume rises during filling; if there ensues an EDV decrease, e.g., with loss of atrial kick in atrial fibrillation, then SV falls too. In systolic dysfunction/failure, a clockwise rotation of the end-systolic pressure-volume line imputes decreased myocardial contractility for the reduced ejection fraction and increased ESV. *Top panels*: in systolic dysfunction, the increased ESV augments the CDL and depresses the diastolic filling vortex strength, leading to filling impairment. Through the increased ESV and superimposed filling impairment, a primary systolic dysfunction/failure can beget supplementary diastolic filling impairment/dysfunction, increasing the need for compensatory mechanisms for maintenance of SV and/or CO. Conversely, diastolic dysfunction with impaired chamber filling can lead directly to a preload-dependent stroke volume curtailment. EDV=end-diastolic volume; ESV=end-systolic volume; SV=stroke volume; CO=cardiac output; CDL=convective deceleration load; VXS=diastolic vortex strength.

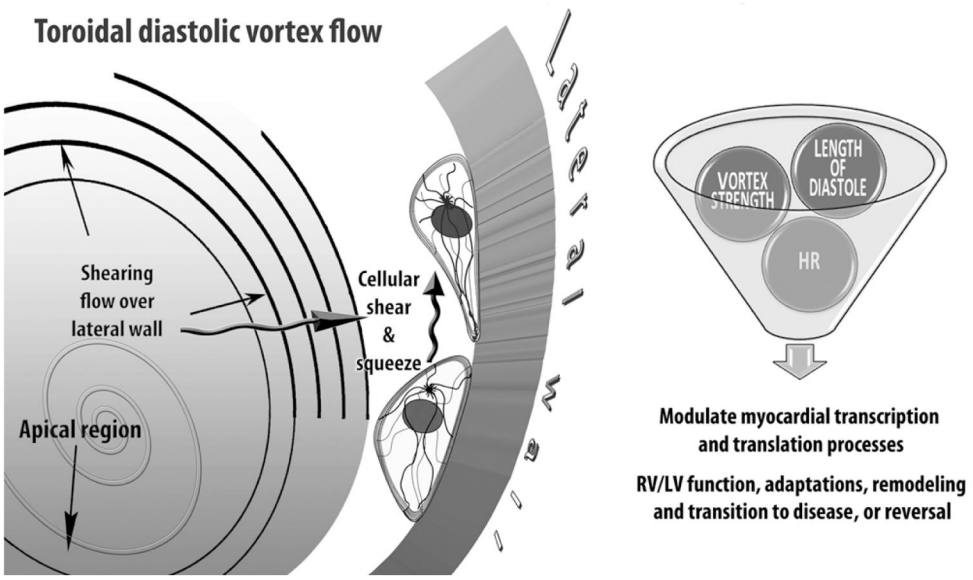

Fig. 7.

Epigenetic dynamic actions of the RV/LV diastolic toroidal vortex: cellular components of the myocardial walls react to their physical 3-D "environment," including variable diastolic vortical shear and "squeeze" forces, by transducing mechanical deformations and forces into differentiated transcription and translation signals, which can adjust myocardial cellular and extracellular tissue and ventricular structure. Mechanosensitive controls modulate cardiomyocyte shape and intracellular architecture, and processes as diverse as proliferation, hypertrophy, and apoptosis, involved in cardiac homeostasis and adaptations. (Reproduced, slightly modified, from Pasipoularides [77] by permission of The Hellenic Cardiological Society.)

Table 1

Isovolumic relaxation dynamics.

		P_0 (mmHg)	P_b (mmHg)	τ (ms)
Condition (Mean ± SD)	Control	13.1 ± 5.1	0.28 ± 1.8	27.8 ± 3.9
	PO	56.2 ±19.1	−7.9 ± 1.5	57.1 ± 2.8
	VO	11.3 ± 5.1	5.3 ± 2.9	26.8 ± 6.1
	IS	9.0 ± 3.5	−1.95 ± 1.1	41.4 ± 13.0
ANOVA	F-statistic	43.33	51.62	31.81
	P-value	0.0001	0.0001	0.0001
P_{BONF}* =0.0167	PO vs. Cl	**0.0001**	**0.0001**	**0.0001**
	VO vs. Cl	0.2295	**0.0001**	0.3140
	IS vs. Cl	0.0355	**0.0038**	**0.0004**

SD, Standard deviation; PO, pressure overload; VO, volume overload; IS, ischemia. Values significantly different from control are presented in boldface.*ANOVA with BONFERRONI's inequality. For the 3 comparisons, a conservative critical value for the modified t-statistics is given using a significance level, P_{BONF}, of (P/3) = (0.05/3) = 0.0167. (Reproduced from Pasipoularides et al. [18] by permission of The American Association for Thoracic Surgery.)

Table 2

Myocardial compliance.

		MC_{max} (kPa^{-1})	P_{MCmax} (Pa)	M_{Ced} (kPa^{-1})	P_{MCed} (Pa)
CONDITION (Mean ± SD)	Cl	0.7276 ± 0.217	315 ± 226	0.0466 ±0.0633	773± 346
	PO	**0.2850± 0.382**	**1,507 ± 785**	0.0235± 0.0254	**2,427 ± 973**
	VO	**0.502 ± 0.263**	137 ± 168	**0.1770 ± 0.1935**	760 ± 453
	IS	**0.502 ± 0.120**	352 ± 227	0.0563 ± 0.0689	680 ± 187
ANOVA	F-statistic	5.02	18.73	3.38	18.52
	P-value	0.0060	0.0001	0.0306	0.0001
	PO vs. Cl	**0.0016**	**0.0001**	0.2020	**0.0001**
P_{BONF} = 0.0167	VO vs. Cl	**0.0232**	0.0407	**0.0131**	0.4768
P_{HOLM} = 0.0250	IS vs. Cl	**0.0102**	0.3619	0.3731	0.2714

Values are means ± SD. MC_{max}, maximum right ventricular (RV) myocardial compliance; P_{MCmax}, RV passive filling pressure at MC_{max}; MC_{ed}, end-diastolic RV myocardial compliance; P_{MCed}, RV passive filling pressure at MC_{ed} (end diastolic). Bold values are significantly changed from CL. (Reproduced from Pasipoularides et al. [19] by permission of The American Physiological Society.)

J Cardiovasc Transl Res. Author manuscript; available in PMC 2014 August 01.